

Diffuse interstellar bands in the spectra of massive YSOs

René D. Oudmaijer, Graeme Busfield, Janet E. Drew

Imperial College of Science, Technology and Medicine, Blackett Laboratory, Prince Consort Road, London, SW7 2BZ, U.K.

received, accepted

ABSTRACT

We have compared the $B-V$ colour excess, $E(B-V)$, obtained for a sample of five optically visible massive YSOs both from diffuse interstellar bands (DIBs) in their spectra and from their optical continuum slopes. Our targets are HD 200775, BD+40°4124, MWC 1080, MWC 297 and MWC 349A. First, $E(B-V)$ towards each of the targets is derived by dereddening the observed continua to match those of B-type standard stars. A survey of DIBs in the spectra of the massive YSOs, and a control field star, then reveals that the DIBs are significantly weaker in the former than would be expected based on the total $E(B-V)$ values. This result is strengthened by the finding that the DIBs in the control field star, HD 154445, have on average the strength expected from its continuum $E(B-V)$.

A rough estimate of the foreground reddening of intervening diffuse interstellar medium shows it to be smaller than the DIB- $E(B-V)$, implying that at least part of the DIB carriers are formed within the parental molecular clouds in which the YSOs are embedded. The formation efficiency of the DIBs varies strongly however from cloud to cloud. The DIB- $E(B-V)$ compares favourably with the total $E(B-V)$ towards BD+40°4124, but is almost negligible in the line of sight towards MWC 297. Despite this general, but not unexpected, deficit we provide evidence that the DIB at 5849Å is a good tracer of total extinction in these lines of sight.

Key words: stars: circumstellar matter – stars: emission line, Be – stars: pre-main sequence – ISM: dust, extinction – ISM: molecules

1 INTRODUCTION

Still unidentified, diffuse interstellar bands (DIBs) are believed to be the result of the absorption of starlight by complex molecules or small dust particles in the interstellar medium. The weak absorption features have been well documented by early spectroscopists although it was not until the 1930s that the interstellar nature of the lines was recognised by Merrill (1934) and coworkers. Continuing investigations showed that the strength of the interstellar absorption features increased with the star’s distance and degree of interstellar reddening (Merrill, 1936). Hence the measurement of the strength of the DIBs is related to path length through the diffuse interstellar medium (ISM). More recently it has become clear that the strength of the DIBs correlate with the column density of HI, but not with the H₂ column (Herbig 1993, 1995).

Although the line strengths of individual DIBs correlate relatively well with the foreground reddening in cases where the diffuse ISM is the main contributor to the extinction, there are particular classes of sightline where this correlation breaks down. For example, for lines of sight through circum-

stellar material the DIB-derived colour excesses ($E(B-V)$) turn out to be smaller than the total $E(B-V)$ determined by other means (e.g. Snow & Wallerstein, 1972; Le Bertre & Lequeux, 1993 on mass-losing objects; Porceddu, Benvenuti & Krelowski 1992, on Be stars). A similar effect has been found for sightlines into star-forming regions, with the further complication that not all DIBs suffer the same reduction (e.g. Meyer & Ulrich 1984, who studied T Tau objects; Adamson et al. 1991, Taurus dark clouds; Jenniskens, Ehrenfreund & Foing 1994, Orion). These findings suggest that the physical conditions in these media are such that the carriers responsible for the DIB absorption do not exist in the same relative quantities as in the diffuse ISM, which is probably related to the formation, excitation and destruction of different DIB carriers. The concept of different DIB ‘families’ (Krelowski & Walker, 1987) can be traced back to this concept. Some band strengths are well correlated with each other, but not with the reddening, while other bands correlate strongly with reddening.

In the present study we describe the behaviour of the DIBs in the lines of sight towards massive young stellar objects. Our targets are the optically visible young stellar ob-

ject (YSO) MWC 349A and four Herbig Be stars, objects which are optically bright enough to obtain high signal-to-noise spectra at intermediate dispersion in the optical. The Herbig Ae/Be stars are widely believed to be associated with circumstellar envelopes of dust. The material in the line of sight towards these young massive objects is thus a combination of ‘normal’ intervening diffuse interstellar material, possibly cold material in the clouds in which the objects have formed, and certainly warm circumstellar material. It is hard to estimate the relative contributions to the total extinction of these media, but observations of the DIBs can in the long run help to elucidate this problem.

Here, we investigate whether the DIBs in the spectra of our targets would imply the same extinction as that derived by other means. Any difference between the derived $E(B-V)$ values would set an upper limit to the contribution of diffuse material to the line-of-sight extinction. In the following we will derive $E(B-V)$ by comparing the observed slopes in the target spectra with standard star spectra - a ‘continuum method’, and derive $E(B-V)$ from the DIB strengths alone using published relations between the EW of DIBs and $E(B-V)$.

The lay-out of this paper is as follows: In Sec.2 we describe the observations and data reduction. In Sec. 3 the determination of the continuum reddening towards the targets is presented and compared with values in the literature. In Sec. 4 the measurement and analysis of the DIBs in the spectra are presented. We then compare the DIB derived $E(B-V)$ with statistical estimates of the colour excess attributable to the foreground ISM described in Sec. 5. The paper ends with a summary.

2 OBSERVATIONS AND DATA REDUCTION

In the course of our study of the optical spectra of massive YSOs (e.g. Drew et al. 1997) we obtained observations on the nights of the 20th to the 22nd June 1994 with the William Herschel Telescope (WHT) at the La Palma Observatory. The weather throughout the run was good, yielding a seeing of 0.7 to 1 arcsec. The twin-beam intermediate dispersion spectrograph (ISIS) was used with the R1200B and R1200R gratings on the blue and red arms of the instrument. The blue detector was a 1124×1124 pixel TEK1 chip, the red detector was a 1180×1280 EEV6 chip. The wavelength ranges covered were 3860–5190Å in the blue arm with a small gap of 120Å between 4270–4390Å. The red arm covered the wavelength range 5840–8390Å. The dichroic crossed over at 5400Å. The instrumental set-up does not allow for the observation of the well-known DIBs at 5780 and 5797 Å. However, the large wavelength coverage and high sensitivity of the observations make up for this loss. For wavelength calibration a copper-neon-argon lamp was observed at frequent intervals. The projected entrance slit width was 1 arcsec, which resulted in spectral resolution elements of 0.8Å ($\lambda/\Delta\lambda \sim 8200$ at $H\alpha$), as determined from arc line profile fits. To minimise cosmic ray events in the spectra, exposure times were limited to 1800s. The observations included a spread of spectral type standards which are listed in Table 1. The typical integration times for these bright stars were of order minutes per setting, resulting in SNR ratios in the continuum of more than 100. Table 2 lists the YSOs

Table 1. The spectral type standards and atmospheric standards.

| Object | SpTp |
|-----------|------------|
| HD 154445 | B1.5V |
| HD 186618 | B0.7IV |
| HD 214432 | B2.5V((n)) |
| HR 6092 | B5IV |
| HR 8335 | B3III |

The spectral types are taken from Walborn (1971)

observed. At each wavelength setting the spectral coverage obtained was generally a few Angstroms in excess of 400Å. The SNR achieved for each of the objects is given in the final column in the tables.

Data reduction was performed using IRAF. Additional manipulation made use of both the IRAF and STARLINK-DIPSO software packages. The data were reduced from two-dimensional frames into a one-dimensional form, through the steps of de-biasing, flat-fielding, sky subtraction and wavelength calibration. A first order cubic spline was used for the wavelength calibration. The fit attained an rms error in the residuals of less than 0.03Å. The extracted spectra were airmass corrected in order to remove the effects of atmospheric extinction in the spectra. We applied the appropriately scaled sum of the wavelength-dependent mean extinction curve for La Palma (King 1985) and the ‘grey’ aerosol component whose magnitude is measured nightly and archived by the Carlsberg Meridian Circle. Where necessary, telluric features were removed by dividing the target star spectra by the corresponding spectra of a suitable comparison star (either HR 6092 or HR 8335). The spectra were scaled such that the depths of the telluric absorption features in the standards match those in the target spectra. The main regions affected by telluric features are 5860–6000Å, 6270–6330Å, 6450–6580Å and 6860Å–6950Å. All wavelengths longwards of 6950Å are susceptible to sporadic atmospheric features.

3 CONTINUUM DETERMINATION OF COLOUR EXCESS.

Before assessing the relation between the DIB strengths and reddening towards the target stars, we need to have an estimate of the *total* $E(B-V)$ for each of them. In this section we will derive $E(B-V)$ by comparing the observed continuum slopes of the spectra with those of spectral standard stars. Their spectra were observed during the same run with the same instrumental set-up. All observations were obtained with the slit at a parallactic angle to minimise the influence of the dispersion of the Earth atmosphere. As stated before, the spectra are corrected for airmass. The procedure is thus independent of the observed flux from the objects, and only takes into account changes in the spectral slopes. It is the same as that used by Cohen et al. (1985) and Drew et al. (1997) to derive the reddening to MWC 349A and MWC 297 respectively, both stars are also included in this sample.

The extracted spectra of the target stars are dereddened to find the best match to the continuum slopes of the standard stars, with $E(B-V)$ as the only free param-

Table 2. Observations of the optically bright YSOs. The effective wavelength coverage was approximately 400Å per setting centred on the wavelengths given in the second column. The co-added SNR is given if more than one observation is available. The B and V magnitudes are taken from Hillenbrand et al. (1992), the V magnitude for MWC 349A is taken from Cohen et al. (1985).

| Object Spectral type | B, V | Wavelength (centre, Å) | Exposure Time (s) | Continuum SNR |
|---------------------------------|--------------|---------------------------|----------------------|------------------|
| HD 200775 B2.5e ¹ | 7.75, 7.42 | 4600 | 50 | 230 |
| | | 5000 | 50 | 250 |
| | | 6055 | 100 | 340 |
| | | 6475 | 30 | 140 |
| | | 6895 | 100 | 390 |
| | | 7315 | 70 | 300 |
| | | 7735 | 40 | 220 |
| BD+40°4124 B3e ¹ | 11.28, 10.54 | 4600 | 1200 | 210 |
| | | 5000 | 600 | 130 |
| | | 6055 | 600 | 190 |
| | | 6475 | 630 | 150 |
| | | 6895 | 200 | 120 |
| MWC 1080 B0 ² | 13.08, 11.68 | 4600 | 2648 | 110 |
| | | 5000 | 1000 | 100 |
| | | 6055 | 1800 | 200 |
| | | 6475 | 200 | 40 |
| | | 6895 | 300 | 110 |
| MWC 297 B1.5Ve ³ | 14.54, 12.17 | 4600 | 9000 | 150 |
| | | 5000 | 1800 | 80 |
| | | 6055 | 5400 | 340 |
| | | 6475 | 2530 | 300 |
| | | 6895 | 2100 | 320 |
| | | 7315 | 1200 | 305 |
| | | 7735 | 500 | 300 |
| MWC 349A | -, 13.5 | 4600 | 5400 | 70 |
| | | 6055 | 800 | 120 |
| | | 6475 | 270 | 115 |
| | | 6895 | 1406 | 205 |
| | | 7315 | 2500 | 355 |

References to the spectroscopic determinations of the spectral types:

¹ : Finkenzeller (1985), ²: Cohen & Kuhi (1979), ³: Drew et al. 1997.

ter. This method implicitly assumes that the intrinsic continuum spectral energy distributions of the Herbig Be stars in the wavelength ranges of interest resemble those of the spectral standards closely. This is indeed the case for our targets. Spectroscopic determinations of their spectral types (Table 2) cover the same spectral type range as our comparison stars (see Table 1). We are not aware of a spectroscopic spectral type for the extreme emission line star MWC 349A - but considering its emission line character and continuum energy distribution, it is widely held to be an early B type star (see e.g. Cohen et al. 1985). The knowledge of the precise spectral type is not critical however, since tests with unreddened Kurucz (1991) models indicate that the differ-

Table 3. Determination of the total $E(B-V)$. The central wavelength of the spectral range is given in column 2. Column 3 records the values of the $E(B-V)$ as determined by the H83 law derived using each of the standard stars. Below the lines of measured $E(B-V)$ s the weighted mean of all the $E(B-V)$ s is presented. Previous $E(B-V)$ or A_V obtained from the literature are given in the final column.

| Object | λ | $E(B-V)$ B0.7,B1.5,B2.5 | Literature | Method |
|------------|-----------|----------------------------|-------------------------|------------|
| HD 200775 | 4600Å | 0.60, 0.45, 0.55 | 0.65 ¹ | colours |
| | 5000Å | 0.75, 0.45, 0.70 | 0.56 ² | colours |
| | | | 0.64 ³ | SED model. |
| | | mean: 0.6 | 0.57 ⁴ | colours |
| | | | | |
| BD+40°4124 | 4600Å | 1.00, 0.85, 0.95 | 0.96 ¹ | colours |
| | 5000Å | 1.15, 0.90, 1.00 | 0.94 ² | colours |
| | | mean: 1.0 | | |
| MWC 1080 | 4600Å | 1.60, 1.45, 1.45 | 1.71 ¹ | colours |
| | 5000Å | 1.80, 1.50, 1.75 | $A_V=5.42$ ⁵ | as here |
| | | mean: 1.6 | | |
| MWC 297 | 4600Å | 2.95, 2.85, 2.95 | 2.68 ¹ | colours |
| | 5000Å | 3.05, 2.70, 2.85 | $A_V=7.9$ ⁶ | NIR slope |
| | | mean: 2.9 | | |
| MWC 349A | 4600Å | 2.95, 2.95, 3.00 | $A_V=9.9$ ⁷ | as here |
| | | mean: 3.0 | $A_V=8.8$ ⁶ | NIR slope |

References: ¹ - Hillenbrand et al. 1992, ² - Finkenzeller & Mundt 1984, ³ - Voshchinnikov, Molster & Thé 1996 ⁴ - Pfau et al. 1987, ⁵ - Cohen & Kuhi 1979, ⁶ - McGregor, Persson & Cohen 1984. ⁷ - Cohen et al. 1985

ence in slopes between the extreme spectral types of O9 and B3 corresponds to an error in the derived $E(B-V)$ of between 0.05 and 0.1, which is much less than our adopted error in the final $E(B-V)$ values.

Additionally, account needs to be taken of the fact that the standard stars are lightly reddened themselves. We derived their reddening using the observed colours (obtained from the SIMBAD database) and intrinsic colours listed in the tables of Schmidt-Kaler (1982) for their respective spectral types. HD 154445 has an $E(B-V)=0.41$, while HD 186618 and HD 214432 display a small amount of reddening of 0.07 and 0.11 respectively. Dereddening HD 154445 with respect to HD 186618 and HD 214432, using the same technique as for the young stellar objects, yielded an $E(B-V)$ difference consistent with the photometric estimates.

Since we are only interested in the continuum slope, strong emission lines (in the Herbig Be stars) and absorption lines (in the standard stars) were snipped out of the spectra to prevent these from affecting the fitting procedure.

Once the spectra had been prepared, the fit procedure was relatively straightforward: each spectrum was dereddened for various values of $E(B-V)$ until an rms minimum between the de-reddened spectrum and the standard star was reached. The procedure encountered too few points upon which to operate satisfactorily in the case of extreme

emission line stars MWC 1080 and MWC349A. In these cases, the colour excesses were better determined by eye.

For the determination of the reddening we have used reddening laws from two sources, the mean $R_V = 3.1$ galactic extinction law compiled by Howarth (1983, H83), and also the R_V dependent analytic prescriptions due to Cardelli, Clayton & Mathis (1989, CCM). The red settings proved not sensitive enough to return useful extinction estimates, and only the results for the 4600 and 5000 Å settings are listed in Table 3.

3.1 Results

The YSO colour excesses, derived using the H83 law, are set out in Table 3. These include the correction for reddening of the standard stars. Below the lines of measured $E(B-V)$ s, the weighted mean of all the $E(B-V)$ s for a given star is presented. As we associate 3σ errors of 0.15 and 0.2 with the 4600 and 5000 Å settings respectively, the weights applied to them in obtaining the mean were chosen to be in the ratio 4:3. It is worthy of note that the derived $E(B-V)$ of MWC 349A and MWC 1080 are in good agreement with the literature values despite the extreme emission line character of their spectra.

In principle the CCM law follows - as the H83 law - the van de Hulst no. 15 law (van de Hulst, 1949) closely for $R_V = 3.1$. The main advantage of the CCM law over the H83 law is that the dependence on the ratio of total to selective reddening may be investigated. It turned out that the R_V sensitivity in our spectra is very small; fits using different values for R_V yielded similar fit qualities and results as those with $R_V = 3.1$. On the whole, the CCM law results were within 1σ of the results outlined in the table. Exceptions to this were obtained for the highly reddened objects MWC 349A and MWC 297 where the CCM law yielded lower $E(B-V)$ values by as much as 0.45 in the 4600 Å setting. This is because the CCM law is somewhat steeper in the 4600 Å wavelength range than the H83 law, a difference that is amplified for highly reddened objects.

4 DIB DETERMINATION OF COLOUR EXCESS

We selected all DIBs listed by Herbig (1995) which appear in the wavelength range covered by our data. The DIBs in Herbig's original list with a normalised equivalent width < 8 mÅ are below our detection capabilities and are not considered. To this list we added stronger lines listed by Jenniskens & Désert (1994, hereafter JD) but not by Herbig (1995). The final list comprises 80 DIBs of which 13 are from the JD catalogue.

With the search list in hand, the spectra were examined independently for DIBs by two of us to minimize the inevitable subjective element. In general, the two independent assessments yielded identifications and equivalent widths that were in agreement at the 10-15% level. In those cases where extreme differences appeared, such as non-identifications or very different equivalent widths, the spectra were inspected again. Often, the combination of faint features and the presence of emission lines in the spectral neigh-

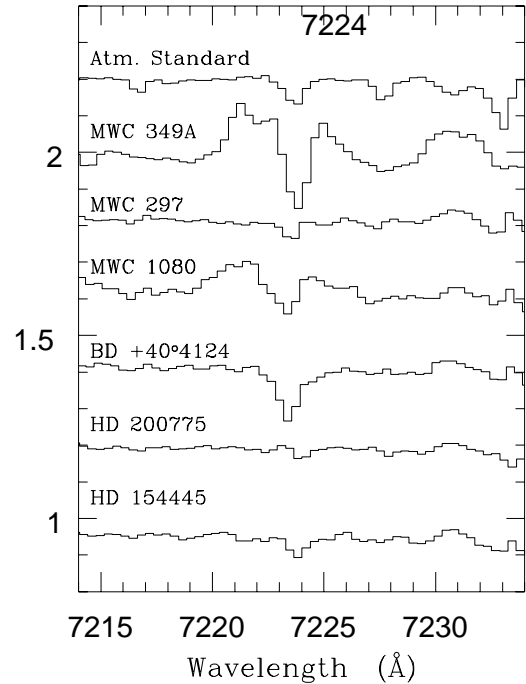
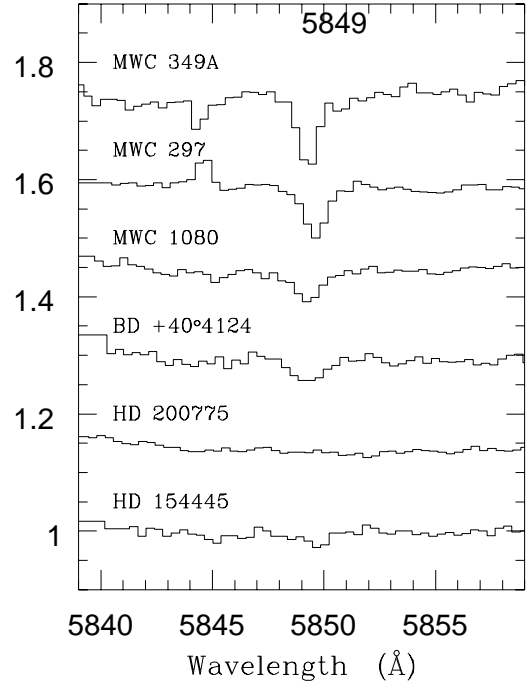


Figure 1. Continuum normalized spectra around the $\lambda 5849$ and $\lambda 7224$ DIBs. The stars are plotted in order of decreasing $E(B-V)$ from top to bottom. The reddened standard star HD 154445 is shown as comparison in both figures. For the $\lambda 7224$ DIB, the atmospheric standard HR 8335 is shown to illustrate results of the correction of telluric absorption lines.

bourhood caused the differences. The measured FWHM are in accordance with their listed values.

Because of the emission line nature of the objects, many lines were hampered by blends with emission lines. The spectral resolution of the observations is in most cases enough to sample the emission lines sufficiently to enable us to distinguish them from the DIBs. After carefully selecting the least affected lines, a sample of 18 DIBs remained. These lines are presented in Table 4. The reddened spectral type standard HD 154445 displays a number of DIBs and is also included in the investigation as a fortuitous control. Examples of two DIBs are given in Fig. 1.

In the following, we will discuss the reddening as traced by the DIBs, and exploit the concept of a DIB- $E(B-V)$. These are calculated using the conversions EW- $E(B-V)$ from JD. Although often the EW- $E(B-V)$ calibration of Herbig (1995) is used, JD provide the mean normalization over four different lines of sight sampling just the diffuse ISM, instead of only one object (HD 183143), which reduces the effect of possible peculiarities in using one particular line of sight. While EW/ $E(B-V)$ for individual DIBs can vary factors of several from sightline to sightline in the data of JD, these variations smooth out to a scatter of 10-20% around the mean when a larger sample of DIBs, such as ours, is considered. This suggests that calculation of $E(B-V)$ from a sample of DIBs gives a good indication of the minimum contribution to the total reddening along the sightline by the diffuse medium (cf. Herbig 1995).

We note in passing that Herbig’s EW values for the DIBs in HD 183143 are larger than those listed by JD. In fact, JD also note that the EW values of HD 183143 presented by Herbig (1975) and Herbig & Leka (1991) ‘may’ be systematically larger by 20%. Le Bertre & Lequeux (1993) also mention that their measurements of the DIBs of HD 183143 ‘possibly give smaller equivalent widths’ than Herbig. We find the same in our own high resolution UES spectrum of HD 183143 (courtesy of Ton Schoenmaker and Eric Bakker).

4.1 Results

The results are summarized in Fig. 2, where the inferred $E(B-V)$ of the DIBs is plotted against the continuum $E(B-V)$ listed in Table 3. Note the panel showing the relation for the $\lambda 5849$ line. It is clear that this line results in deduced $E(B-V)$ values for every star (except for HD 200775 where the line is not detected) which are in agreement with the continuum-determined $E(B-V)$. The spectra around this line are shown in Fig. 1. Our data strengthen the tentative suggestion of Chlewicki et al. (1986) that the $\lambda 5849$ line is frequently a good indicator for the *total* extinction towards an object. A crude match between line- $E(B-V)$ and continuum- $E(B-V)$ also seems to exist for the $\lambda\lambda 4963, 4726$ bands. However, in most other lines, the trend is that the line- $E(B-V)$ value is lower than that determined from the continuum.

An illustrative plot is provided in Fig. 3. It shows the inferred $E(B-V)$ of the measured lines against DIB wavelength. The horizontally drawn lines indicate the continuum $E(B-V)$ (Table 3). In especially BD+40°4124 and the standard star HD 154445, the DIBs return an $E(B-V)$ close to the value of the total $E(B-V)$, but in the other cases it

Table 5. $E(B-V)$ as derived from the DIBs. n is the number of lines used in the calculation

| Star | Cont. $E(B-V)$ | n | DIB < $E(B-V)$ > |
|------------|-------------------|----|---------------------|
| HD 154445 | 0.4 | 15 | 0.43 (0.07) |
| HD 200775 | 0.6 | 9 | 0.14 (0.07) |
| BD+40°4124 | 1.0 | 18 | 0.64 (0.08) |
| MWC 1080 | 1.6 | 17 | 1.01 (0.10) |
| MWC 297 | 2.9 | 18 | 0.47 (0.08) |
| MWC 349A | 3.0 | 16 | 1.56 (0.11) |

can be grasped straightaway that the DIB $E(B-V)$ is significantly smaller than that determined for the continuum. The three DIBs in the spectrum of MWC 297 that are sufficiently strong to trace the total $E(B-V)$ are the same three mentioned above as correlating well with the total $E(B-V)$. All the other DIBs return values very much smaller than the continuum $E(B-V)$.

The mean DIB- $E(B-V)$, calculated from all detected lines is presented in Table 5. In order to avoid a bias towards the larger EWs, the mean has been calculated using a $1/\sigma$ weighting, instead of weighting the measurements according to the inverse square of their errors (the officially commended weighting scheme). We did not take into account any non-detections, but it can be seen in Fig. 3 that the resulting upper limits on inferred $E(B-V)$ values are mostly in agreement with the means obtained.

In the only instance where we are certain that the diffuse ISM is the principal extinction medium, HD 154445, the DIB $E(B-V)$ is in pleasing agreement with the continuum $E(B-V)$. For the massive YSOs, it appears that the DIB- $E(B-V)$ is always smaller than the continuum $E(B-V)$, but that the extent of the shortfall differs substantially from object to object: specifically, for BD+40°4124 the DIB- $E(B-V)$ is about 65% of the continuum $E(B-V)$, while the other extremes are MWC 297 and HD 200775, where the DIBs seem to trace only 20% or less of the total $E(B-V)$.

5 THE CONTRIBUTION OF FOREGROUND REDDENING TO THE TOTAL EXCESS

Now that the total $E(B-V)$ and the $E(B-V)$ traced by the DIBs are derived, it is of interest to have an independent estimate of the extinction due only to the foreground diffuse interstellar medium along our sightlines. This is done by investigating the reddening of nearby field stars.

To facilitate this, we have searched the polarization catalogue compiled by Matthewson et al. (1978), which contains, in combination with polarization data, values for the extinction and photometric distances of more than 7500 objects. For each of our stars, we selected all objects within a radius of 400 arcmin. The results of this exercise are set out in Fig. 4, where the $E(B-V)$ for each star is plotted against its distance modulus $m-M$. A consistency check was made by a comparison with similar relations presented by FitzGerald (1968) and Neckel & Klare (1980), and by calculating the $E(B-V)$ and distance modulus using the spectral types, intrinsic $B-V$, and M_V (using $R_V = 3.1$) listed by Schmidt-Kaler (1982) for randomly selected objects. This

Table 4. The DIBs in the spectra of the 5 massive YSOs and the control star HD 154445. The first two columns identify the DIBs by their wavelength and their respective normalization to unit $E(B-V)$ as published by JD. Errors on the equivalent width are given between brackets. The value for the $\lambda 6203$ DIB is the sum of the 6203 and 6204 Å components resolved by JD, but not by us. NO: Not observed, B: blend with emission line, an indication of the EW is given NP: Not present – in general an upper limit of 10mÅ is found.

| λ Å | W/ $E(B-V)$ mÅ | HD 200775 | HD 154445 | BD+40°4124 | MWC 1080 | MWC 297 | MWC 349A |
|----------------|-------------------|-----------|-----------|-------------|-------------|-------------|-------------|
| 4428 | 2231 | 330 (70) | 890 (80) | 1070 (270) | 1740 (450) | 1790 (360) | 3420 (480) |
| 4726 | 123 | 10 (5) | 65 (10) | 95 (10) | 155 (15) | 315 (55) | 500 (100) |
| 4963 | 16 | NP | 7 (4) | 20 (5) | 26 (2) | 75 (20) | NO |
| 5849 | 48 | NP | 30 (10) | 55 (12) | 75 (10) | 115 (20) | 130 (25) |
| 6089 | 17 | NP | 15 (5) | 15 (5) | 20 (3) | 25 (5) | 50 (10) |
| 6195 | 61 | 20 (10) | 35 (5) | 50 (10) | 75 (10) | 25 (5) | 130 (30) |
| 6203 | 296 | 25 (10) | 65 (10) | 180 (25) | 200 (40) | 60 (25) | 330 (40) |
| 6269 | 137 | NP | 50 (10) | 85 (10) | 90 (15) | 35 (10) | 40 (25) |
| 6376 | 26 | NP | 16 (4) | 20 (5) | 32 (6) | 10 (5) | 95 (8) |
| 6379 | 78 | 12 (5) | 57 (7) | 60 (6) | 93 (10) | 70 (10) | 170 (15) |
| 6613 | 231 | 18 (5) | 120 (15) | 150 (20) | 275 (35) | 115 (15) | 425 (45) |
| 6660 | 51 | NP | 14 (7) | 17 (4) | 50 (20) | 25 (5) | 65 (5) |
| 6843 | 27 | 6 (3) | NP | 22 (10) | 25 (5) | 8 (2) | 38 (5) |
| 6993 | 116 | 50 (10) | 75 (6) | 80 (10) | 65 (25) | 35 (10) | 280 (35) |
| 7119 | 40 | 8 (5) | 22 (5) | 30 (4) | 15 (6) | 13 (3) | 58 (6) |
| 7224 | 259 | NP | 60 (7) | 160 (20) | 140: (B) | 35 (10) | 240: (B) |
| 7357 | 48 | NP | NP | 10 (5) | 30 (10) | NP | 20 (5) |
| 7367 | 42 | NP | NP | 20 (5) | 45 (5) | 20 (5) | 110 (15) |

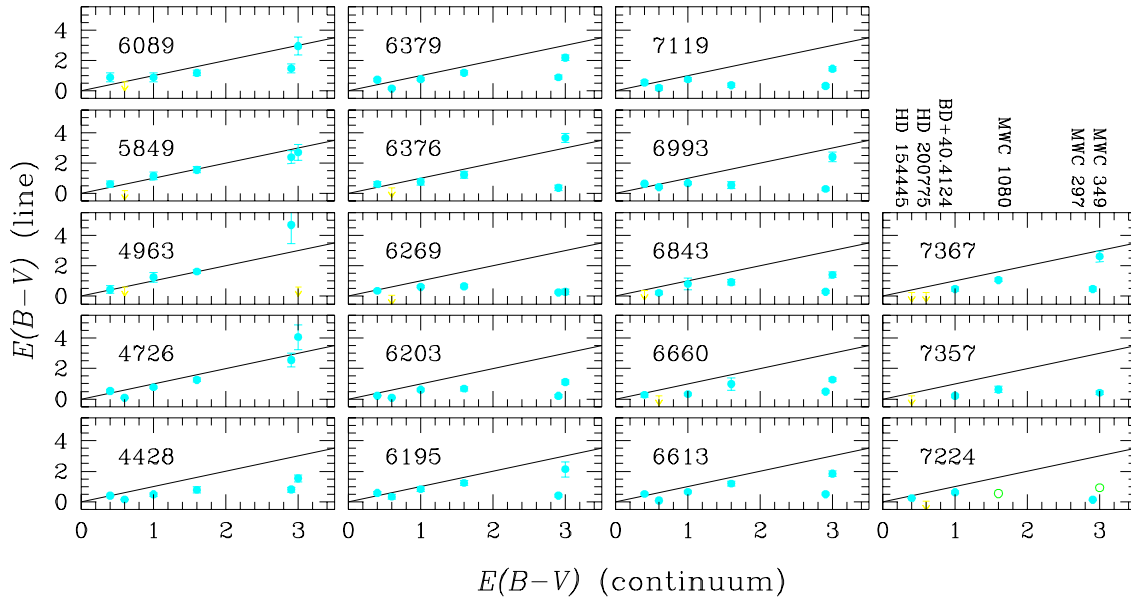


Figure 2. Deduced $E(B-V)$ from the measured EWs of the lines for the different objects plotted per line. The open circles represent the bands affected by emission lines. The solid lines indicate the $E(B-V)$ (DIB) equals the $E(B-V)$ (continuum) relation.

showed that the listed $E(B-V)$ and $m-M$ in the Mathewson et al. (1978) catalogue are in general correct to within 0.2 and 0.5 magnitudes respectively.

In the figure, the objects are indicated with vertical lines

at their estimated distances* and horizontal lines represent-

* The adopted distances to the objects are as follows: MWC 297 at 250 pc based on its spectral type (Drew et al. 1997); MWC 349A - at least 1000 pc, based on spectral type of com-

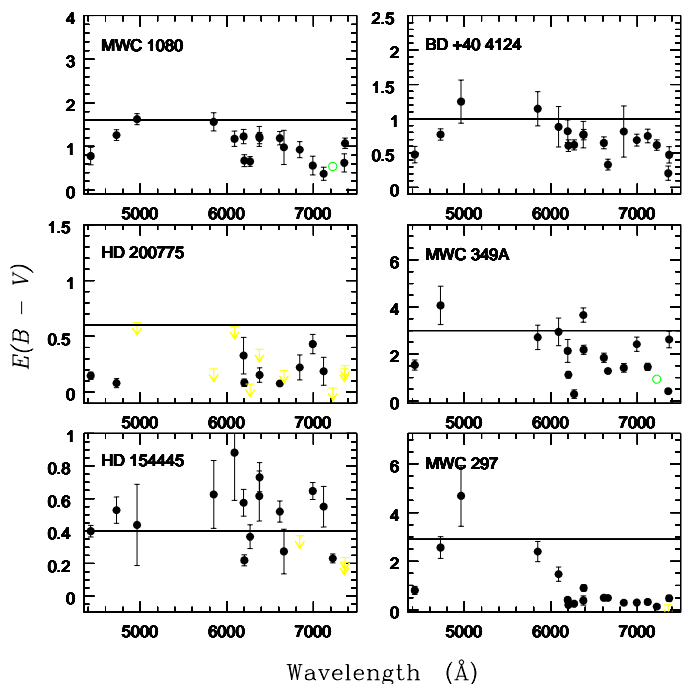


Figure 3. Inferred $E(B-V)$ from the DIBs on a line by line basis. The horizontal lines represent the continuum $E(B-V)$.

ing the DIB- $E(B-V)$. The lines of sight to BD+40°4124, MWC 349A and MWC 1080 initially show a trend between the distance modulus and $E(B-V)$, which then breaks down at large distances, where the objects are scattered in $E(B-V)$. Since all these objects are located in, or near, molecular clouds the scatter is real, and reflects the many stars at different depths and locations within patchy clouds. Where feasible, a conservative upper bound to the foreground reddening in the lines of sight is indicated by the solid lines.

It is not ruled out that the sightlines to MWC 297 and HD 200775 show a similar behaviour to that seen in e.g. MWC 349A, but the sparse number of data points makes it hard to recognize this. For example, MWC 297 is known to be located within the Aquila Rift at a distance of about 250 pc (Dame & Thaddeus, 1985, Drew et al. 1997). However, one may see that it is only beyond ~ 500 parsec ($m-M \sim 8.5$) that the data points scatter in a similar way as for MWC 349A. These stars must be behind the Aquila Rift. It would appear that the catalogue of Matthewson et al. includes too few stars that are located in the Rift at $m-M \sim 6-7$. Similarly, it seems in the figure for HD 200775 (positioned within NGC 7023) that $E(B-V)$ only starts to become significant beyond $m-M \sim 6$.

It is clear that in all cases the foreground extinction is much less than the total extinction towards the objects (Fig. 4, Table 5). For the $E(B-V)$ traced by the DIBs some interesting differences appear. For both MWC 297 and HD 200775 the foreground extinction may be comparable with the $E(B-V)$ as calculated from the DIBS, but not larger. In

panion MWC 349B (Cohen et al. 1985) ; HD 200775, 600 pc by Rogers, Heyer & Dewdney (1995) based on spectral type B2.5IV. BD+40°4124, 1000 pc, Hillenbrand et al. 1995; MWC 1080, 2500 pc, Cantó et al. (1984), but is likely to be smaller - see Hillenbrand et al. (1982), who cite 1000 pc. HD 154445, 275 pc, based on spectral type.

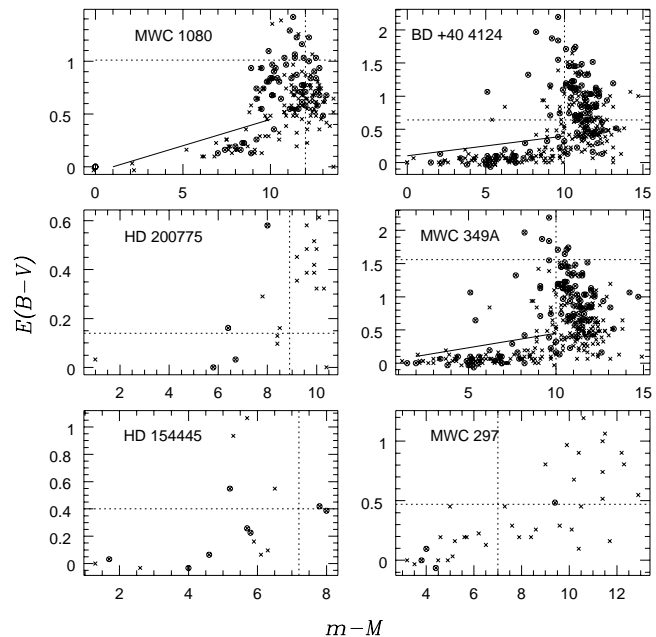


Figure 4. The relationship between $E(B-V)$ and distance modulus of objects around the position of the target stars. The circles indicate objects within 200 arcmin, the crosses represent objects within 400 arcmin. The locations of the target stars are indicated by the intersection of their DIB- $E(B-V)$ and distance. Note that the total $E(B-V)$ to the objects is in all cases larger than the DIB- $E(B-V)$ (Table 5). The solid lines represent a conservative estimate of the contribution of the foreground reddening as a function of distance.

the other cases, the DIB- $E(B-V)$ is intermediate between the total $E(B-V)$ and the foreground extinction. This suggests that the molecular clouds, or even the circumstellar material, harbour conditions in which the DIB carriers can be present albeit at reduced abundance.

We remind however that there is a small collection of DIBs in the spectrum of MWC 297 that is particularly strong; namely $\lambda 5849$, $\lambda 4963$ and $\lambda 4726$ appear to trace the total continuum $E(B-V)$.

6 CONCLUDING REMARKS

DIB features are in general well-correlated with the interstellar extinction for field objects, but deviate in instances where circumstellar or parental cloud material is present. The results in Table 5 and in the previous section certainly indicate that the latter is true for our sample of massive YSOs as well. The diffuse ISM contributes only a fraction of the total reddening towards the YSOs – the rest of the extinction being due to either cloud or circumstellar material.

In conclusion, our study of Diffuse Interstellar Bands towards a sample of massive YSOs can be summarized as follows:

- (i) From our crude estimates of the foreground extinction we find that a large fraction of the extinction to these stars is not provided by the diffuse interstellar medium, but by circumstellar material or dust within the parental cloud.
- (ii) By and large, the DIB- $E(B-V)$ is smaller than the

total $E(B-V)$ towards the optically visible massive YSOs - but is mostly larger than the expected foreground reddening. This means that at least a fraction of the DIBs are formed within the molecular clouds, but less efficiently than in the normal diffuse ISM. This implies that conditions in this material are such that DIB excitation is weaker or that the DIB carriers are less efficiently formed or more prone to destruction. The DIBs trace most of the $E(B-V)$ suffered by BD+40°4124 but very little in the line of sight to MWC 297. Such variations in ‘efficiency’ clearly imply that the conditions vary strongly from one cloud of massive star formation to the other.

(iii) If the DIBs are due to different types of carrier, the strength of the lines will be proportional to the respective column densities of the carriers. The effective normalization of line-strengths to $E(B-V)$ for ‘normal’ diffuse interstellar material then gives us a handle on their relative abundances. From the fact that the $\lambda 5849$ line seems to trace the total $E(B-V)$, one may infer that the carrier of this line is more readily formed or less likely to be destroyed, in star-forming clouds than other lines. The same may also be true for the $\lambda 4726$ and $\lambda 4963$ DIBs as strikingly illustrated by the case of MWC 297.

Acknowledgments Kaylene Murdoch and Phil Lucas are thanked for obtaining the observations. The allocation of time on the WHT was awarded by PATT, the United Kingdom allocation panel. This work was entirely funded by the Particle Physics and Astronomy Research Council of the United Kingdom.

REFERENCES

- Adamson A.J., Whittet D.C.B., Duley W.W. 1991, MNRAS 252, 234
- Cantó, J., Rodríguez, L.F., Calvet, N., Levreault, R.M. 1984, ApJ 282, 631
- Cardelli J.A., Clayton G.C., Mathis J.S. 1989, ApJ 345, 245
- Chlewicki G., van der Zwet G.P., van IJzendoorn L.J., Greenberg J.M. 1986 ApJ 305, 455
- Cohen M., Biegging J.H., Dreher J.W., Welch W.J. 1985, ApJ 292, 249
- Cohen M., Kuhi L. 1979, ApJS 41, 743
- Dame T. M., Thaddeus P. 1985, ApJ 297, 751
- Drew J.E., Busfield G., Hoare M.G., Murdoch K.A., Nixon C.A., Oudmaijer R.D. 1997, MNRAS 238, 538
- Finkenzeller U. 1985, A&A 151, 340
- Finkenzeller U., Mundt R. 1984, A&AS 55, 109
- FitzGerald M.P. 1968, AJ 73, 983
- Herbig G.H. 1975, ApJ 196, 127
- Herbig G.H. 1993, ApJ 407, 142
- Herbig G.H. 1995, ARA&A 33, 19
- Herbig G.H., Leka K.D. 1991, ApJ 382, 193
- Hillenbrand L.A., Strom S.E., Vrba F.J., Keene J. 1992, ApJ 397, 613
- Hillenbrand, L.A., Meyer, M.R., Strom, S.E., Skrutskie, M.F. 1995, AJ 109, 280
- Howarth I.D. 1983, MNRAS 203, 301
- Jenniskens P., Désert, F.-X. 1994, A&AS 106, 39
- Jenniskens P., Ehrenfreund P., Foing B. 1994, A&A 281, 517
- King D.L. 1985, RGO/La Palma Technical Note No. 31
- Krelowski J., Walker G.A.H. 1987, AJ 312, 860
- Kurucz R.L. in *Precision Photometry: Astrophysics of the Galaxy*, ed. A.C. Davis Philip, A.R. Uggren, K.A. James, Schenectady: Davis, p 27
- Le Bertre T., Lequeux J. 1993, A&A 274, 909
- Matthewson D.S., Ford V.I., Klare G., Neckel T., Krautter J. 1978, Bull. Inf. CDS, 14, 115
- McGregor P.J., Persson S.E., Cohen J.G. 1984, ApJ 286, 609
- Merrill P.W. 1934, PASP 46, 206
- Merrill P.W. 1936, ApJ 83, 126
- Meyer D.M., Ulrich R.K. 1984, ApJ 283, 98
- Neckel Th., Klare G. 1980, A&AS 42, 251
- Pfau W., Piirola V., Reimann H.-G. 1987, A&A 179, 134
- Porceddu I., Benvenuti P., Krelowski J. 1992, A&A 257, 745
- Rogers C., Heyer M.H., Dewdney P.E. 1995, ApJ 442, 694
- Schmidt-Kaler Th., 1982, in Schaifers, K., Voigt, H.H., eds, Landolt-Börnstein New Series, Vol. 2b. Springer-Verlag, Berlin.
- Snow T.P., Wallerstein G. 1972, PASP 84, 492
- van de Hulst H.C. 1949, Physica 15, 740
- Voshchinnikov N.V., Molster F.J., Thé P.S. 1996, A&A 312, 243
- Walborn N. R. 1971, ApJS, 23, 257